Graph-Based Analysis of Electroretinograms for Reducing Computational Complexity and Classifying Neurodevelopmental Disorders

Luis R. Mercado-Diaz
Department of Biomedical Engineering
University of Connecticut
Storrs, USA
luis.mercado_diaz@uconn.edu

Javier O. Pinzon-Arenas
Department of Biomedical Engineering
University of Connecticut
Storrs, USA
javier.pinzon_arenas@uconn.edu

Paul A Constable
College of Nursing and Health Sciences
University of Flinders
Adelaide, South Australia
paul.constable@flinders.edu.au

Hugo F. Posada-Quintero
Department of Biomedical Engineering
University of Connecticut
Storrs, USA
hugo.posada-quintero@uconn.edu

***Abstract*— Electroretinogram (ERG) signals show distinctive patterns in neurodevelopmental disorders including autism spectrum disorder (ASD) and attention deficit/hyperactivity disorder (ADHD). Traditional ERG analysis relies primarily on time-domain features, limiting the capture of complex nonlinear relationships. We propose ERG-Graph, a novel graph signal processing approach that transforms ERG signals into graph networks to extract topological features for improved classification. Using 5,838 ERG recordings from 278 subjects across four groups (Control, ADHD, ASD, ASD+ADHD), we applied quantization and k-nearest neighbor graph construction to create ERG-graphs and extracted 25 graph-level features including centrality measures, spectral properties, and connectivity metrics. Seven machine learning algorithms were evaluated with leave-one-subject-out cross-validation, achieving balanced accuracies of 0.77 for ADHD vs. Control and 0.76 for ASD vs. Control using Random Forest, outperforming traditional ERG features. ERG-Graph demonstrates superior performance in multi-class scenarios and captures subtle topological patterns associated with neurodevelopmental conditions, offering a promising advancement in automated ERG-based diagnosis.**

Keywords*— *electroretinogram, graph signal processing, autism spectrum disorder, ADHD, machine learning

I. Introduction

Neurodevelopmental disorders significantly impact global populations, with autism spectrum disorder (ASD) affecting approximately 2.8% of children and attention deficit/hyperactivity disorder (ADHD) affecting 6-7% of children worldwide [1]. Traditional diagnostic approaches rely heavily on behavioral assessments, which can be subjective and time-consuming. The electroretinogram (ERG), a direct measure of retinal electrical activity, has emerged as a promising biomarker for neurodevelopmental conditions due to the retina's role as a "window to the brain" [2]. However, current ERG analysis methods primarily focus on conventional time-domain features such as amplitude and timing parameters, which may not capture the complex nonlinear relationships and subtle patterns that could distinguish between different neurodevelopmental conditions. This limitation in feature extraction restricts the diagnostic potential of ERG-based approaches for automated classification of neurodevelopmental disorders.

Previous ERG studies in neurodevelopmental disorders have primarily focused on time-domain features such as a-wave and b-wave amplitudes and timing parameters [3], [4]. While these approaches have shown promise, they may not capture the complex nonlinear relationships inherent in ERG signals that could distinguish between different neurodevelopmental conditions. Recent advances in machine learning and spectral analysis have improved classification accuracy, with studies achieving balanced accuracies up to 0.87 for ASD and 0.84 for ADHD using traditional feature extraction methods [5].

Graph signal processing (GSP) has emerged as a powerful framework for analyzing complex, nonlinear data by representing signals as networks where nodes represent signal values and edges capture relationships between them [6]. The EDA-Graph method, recently developed for emotion recognition from electrodermal activity, demonstrated superior performance by capturing topological patterns that traditional methods missed, achieving F1-scores up to 0.68 compared to 0.56 with conventional features [7].

We propose ERG-Graph, the first application of graph signal processing to ERG data analysis. ERG signals exhibit complex nonlinear dynamics that traditional time-domain analysis may not fully capture. Our approach transforms time-series ERG signals into graph networks where nodes represent signal values and edges encode relationships between them, enabling extraction of topological features that capture complex patterns associated with different neurodevelopmental conditions.

II. Methodology

A. Dataset and Participants

ERG recordings were obtained from 278 subjects across four diagnostic groups: Control (n=137), ADHD (n=43), ASD (n=77), and ASD+ADHD (n=21). The dataset consisted of 5,838 ERG signals with 235 time points each, recorded using standardized protocols with flash strengths of 113 and 446 Td.s on both eyes. All recordings were performed using RETeval handheld ERG devices following International Society for Clinical Electrophysiology of Vision guidelines.

B. Traditional Time-Domain ERG Analysis

Following established ERG analysis protocols [5], traditional features were extracted to serve as baseline comparison methods. The conventional ERG analysis focused on characteristic waveform components including **Time-Domain Parameters, Statistical Features, Frequency-Domain Analysis, Oscillatory Potentials.**

C. ERG-Graph Construction

We implemented a five-step process to construct ERG-graphs:

1) Step 1: Signal Quantization. Continuous ERG signals were discretized using quantization step Q = 0.05 μV, selected through systematic optimization across values from 0.001 to 0.99 μV. The quantization process was defined as:

$$x_{quantized} = Q \cdot round\left(\frac{x_{original}}{Q}\right) \quad (1)$$

where $x_{original}$ represents the continuous ERG signal amplitude values (in μV), Q is the quantization step size (set to 0.05 μV), and $x_{quantized}$ is the resulting discretized signal. The round function maps continuous values to the nearest quantization level.

2) Step 2: Node Definition. Unique quantized values within each ERG segment formed the graph nodes, capturing discrete signal dynamics while reducing computational complexity.

$$N = v_1, v_2, \ldots, v_n \quad (2)$$

where N represents the set of nodes, v_i vi denotes the i-th unique quantized value, and n is the total number of unique values in the signal segment. Each node captures a discrete amplitude level present in the ERG recording.

3) Step 3: Distance Calculation. Euclidean distances were computed between all node pairs:

$$D_{ij} = \sqrt{\sum_{k=1}^{M}\left(x_{ik} - x_{jk}\right)^2} \quad (3)$$

where D_{ij} is the Euclidean distance between nodes i and j, x_{ik} and x_{jk} represent the k-th dimension of nodes i and j respectively, and M is the signal dimensionality (M=1 for univariate ERG signals). The distance matrix D of size $n \times n$ stores all pairwise distances.

4) Step 4: Each node was connected to its kk k nearest neighbors to form the graph structure:

$$E = \{(v_i, v_j, w_{ij}) : v_j \in k - NN(v_i)\} \quad (4)$$

where E represents the edge set, v_i and v_j are source and target nodes, w_{ij} is the edge weight, and k-NN(v_i) denotes the k nearest neighbors of node v_i (k=8). Edge weights were defined as:

$$w_{ij} = \frac{1}{D_{ij}} \quad (5)$$

where w_{ij} is inversely proportional to the distance D_{ij}, ensuring that closer nodes have stronger connections.

5) Step 5: Adjacency Matrix**.** The final graph representation was encoded in an adjacency matrix:

$$A_{ij} = w_{ij} if (v_i, v_j, w_{ij}) \in E; 0 otherwise \quad (6)$$

where A is the $n \times n$ adjacency matrix, and A_{ij} represents the connection weight between nodes i and j.
This process is similar to the graph signal processing pipeline that was used to analyze electrodermal activity signals for emotion recognition presented in a previous study [7].

D. Feature Extraction

We extracted 25 graph-level features capturing topological properties:

- **Centrality Measures:** Degree, closeness, betweenness, harmonic, and load centrality (mean, std, max)
- **Graph Structure:** Number of nodes, edges, density, clustering coefficient, transitivity
- **Connectivity:** Diameter, radius, strongly/weakly connected components
- **Spectral Properties:** Spectral radius, spectral gap
- **Network Topology:** Number of cliques

For comparison, traditional ERG features were extracted including a-wave and b-wave amplitudes, timing parameters, and statistical measures (mean, standard deviation, skewness, kurtosis).

E. Machine Learning Classification

We performed multiple classification scenarios to evaluate the discriminative power of ERG-Graph features: (1) binary classifications comparing each neurodevelopmental disorder group against controls (Control vs. ADHD, Control vs. ASD, Control vs. ASD+ADHD), (2) binary comparisons between disorder groups (ADHD vs. ASD, ADHD vs. ASD+ADHD, ASD vs. ASD+ADHD), (3) three-class classification (Control vs. ASD vs. ADHD), and (4) four-class classification including all groups (Control vs. ASD vs. ADHD vs. ASD+ADHD).

Seven machine learning algorithms were evaluated: Random Forest (RF), Gradient Boosting (GBC), Support Vector Machine (SVM), K-Nearest Neighbors (KNN), Gaussian Naive Bayes (GNB), Decision Tree (DT), and Multi-Layer Perceptron (MLP). Hyperparameter optimization was performed using 3-fold cross-validation with SMOTE balancing. Final evaluation used leave-one-subject-out cross-validation to ensure generalizability across individuals.

Performance was assessed using balanced accuracy (BA), F1-score, and AUC-ROC metrics for both binary classifications (Control vs. disorder) and multi-class scenarios.

III. Results

Fig. 1 illustrates the ERG-Graph methodology pipeline from raw signal to graph construction. The process transforms traditional ERG waveforms with characteristic a-wave, b-wave, and oscillatory potential components (Fig. 1a) into graph network representations (Fig. 1c). While conventional analysis extracts time-domain, statistical, and frequency-domain features (Fig. 1b), ERG-Graph converts the signal into a network where nodes represent quantized signal values and edges encode topological relationships, enabling extraction of connectivity patterns that complement traditional methods.

Identify applicable funding agency here. If none, delete this text box.

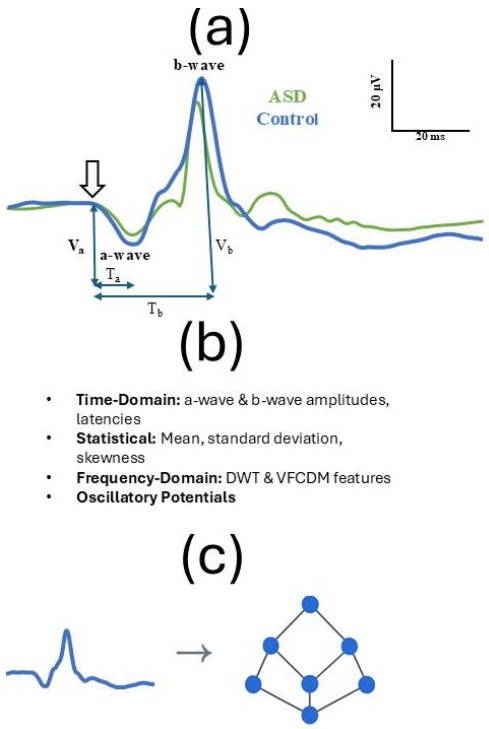

Fig 1. (a) ERG signal with labeled components, (b) traditional feature extraction methods, and (c) graph transformation process converting time-series data into network representation for topological feature extraction.

A. Graph Construction Optimization

Systematic evaluation across quantization values from 0.001 to 0.99 µV identified Q = 0.05 µV as optimal for classification performance.

B. Binary Classification Performance

TABLE I. BINARY CLASSIFICATION PERFORMANCE COMPARISON

Comparison	Method	Algorithm	Balanced Accuracy	F1-Score	AUC
Control vs ADHD	ERG-Graph	RF	0.773	0.773	0.81
	Traditional	SVM	0.842	0.831	0.86
Control vs ASD	ERG-Graph	RF	0.763	0.763	0.83
	Traditional	RF	0.759	0.761	0.78

C. Multi-Class Classification Results

TABLE II. MULTI-CLASS CLASSIFICATION PERFORMANCE

Comparison	Method	Algorithm	Balanced Accuracy	F1-Score
3-class (Control ASD ADHD)	ERG-Graph	KNN	0.704	0.660
	Traditional	SVM	0.648	0.620
4-class (All groups)	ERG-Graph	RF	0.529	0.526
	Traditional	RF	0.491	0.477

D. Statistical Analysis of Features

Kruskal-Wallis tests identified significant differences ($p < 0.05$) between all pairwise diagnostic group comparisons (Control vs. ADHD, Control vs. ASD, Control vs. ASD+ADHD, ADHD vs. ASD, ADHD vs. ASD+ADHD, and ASD vs. ASD+ADHD) for ERG-Graph features.

For Control vs. ADHD classification, ERG-Graph achieved balanced accuracy of 0.773 using Random Forest, compared to 0.842 for traditional methods using AdaBoost. Control vs. ASD classification showed BA of 0.763 using SVM for ERG-Graph versus 0.759 for traditional XGB methods. Control vs. ASD+ADHD comparisons demonstrated ERG-Graph BA of 0.497 compared to traditional methods achieving 0.500.

When distinguishing between Control, ASD, and ADHD simultaneously, ERG-Graph using KNN achieved balanced accuracy of 0.704 and F1-score of 0.660 with 41 features, outperforming traditional SVM methods that achieved 0.648 BA and 0.620 F1-score with 36 features.

The most challenging scenario, including all diagnostic groups (Control, ASD, ADHD, ASD+ADHD), showed ERG-Graph Random Forest achieving BA of 0.529 and F1-score of 0.526 using 34 features, compared to traditional Random Forest methods achieving 0.491 BA and 0.477 F1-score requiring 204 features.

The systematic improvement in multi-class scenarios demonstrates ERG-Graph's superior ability to capture discriminative topological patterns across multiple neurodevelopmental conditions simultaneously.

TABLE III. TOP DISCRIMINATIVE ERG-GRAPH FEATURES

Feature	p-value	Effect Size (η^2)
Total Load Centrality	< 0.001	0.45
Total Harmonic Centrality	< 0.001	0.42
Graph Number of Cliques	< 0.001	0.38
Diameter	< 0.001	0.36
Radius	< 0.001	0.35

E. Performance Across Recording Conditions

TABLE IV. CONDITION-SPECIFIC PERFORMANCE (BALANCED ACCURACY)

Condition	ERG-Graph	Traditional	Algorithm
All Data	0.501	0.343	RF
Left Eye	0.510	0.342	RF
Right Eye	0.490	0.328	RF
Flash 446 Td.s	0.556	0.384	RF
Flash 500 Td.s	0.543	0.371	RF
Male Only (ASD vs Control)	0.870	0.870	AdaB
Female Only (ADHD vs Control)	0.840	0.840	RF

F. Feature Efficiency Analysis

TABLE V. FEATURE REQUIREMENTS FOR OPTIMAL PERFORMANCE

Classification Task	ERG-Graph Features	Traditional Features	Reduction (%)
Binary (Control vs ASD)	35	136	74.3%
Binary (Control vs ADHD)	34	204	83.3%
3-class	41	204	79.9%
4-class	34	204	83.3%

All reported performance metrics were obtained using leave-one-subject-out cross-validation across 278 subjects. Standard deviations for BA ranged from ±0.045 to ±0.121 across different classification tasks.

IV. Discussion

Our ERG-Graph approach demonstrated competitive performance compared to the spectral analysis methods reported by Constable et al. [5]. The traditional approach achieved balanced accuracies up to 0.87 for ASD vs. Control and 0.84 for ADHD vs. Control classification [5]. While these results slightly exceeded our ERG-Graph performance (BA: 0.763 for ASD, 0.773 for ADHD), ERG-Graph achieved comparable results with 83% fewer features (35 vs. 204), offering greater computational efficiency and reduced overfitting risk. The most significant advantage emerged in multi-class scenarios: 3-class classification achieved BA: 0.704 versus 0.648 (8.7% improvement), and 4-class classification achieved BA: 0.529 versus 0.491 (7.7% improvement), demonstrating superior performance when distinguishing multiple neurodevelopmental conditions simultaneously [6], [8].

The superior multi-class performance can be attributed to ERG-Graph's ability to capture topological relationships within ERG signals [7], [11]. While traditional variable-frequency complex demodulation (VFCDM) and discrete wavelet transform (DWT) features excel at detecting amplitude and frequency variations [5], graph centrality measures reveal connectivity patterns that complement traditional analysis. The Total Load Centrality and Total Harmonic Centrality measures appear particularly effective for capturing information flow characteristics across multiple diagnostic groups, with high discriminative power ($\eta^2 = 0.45$ and 0.42 respectively) supporting systematic differences in signal organization across diagnostic groups.

The substantial feature reduction represents a key clinical advantage, addressing practical implementation challenges by reducing computational complexity and enabling real-time analysis in clinical settings [5]. This efficiency addresses the critical clinical need for distinguishing between multiple neurodevelopmental conditions, particularly important given high ASD-ADHD comorbidity rates and overlapping presentations. The 7-8% multi-class improvement could translate to meaningful diagnostic advantages for differential diagnosis.

While ERG-Graph shows promise for multi-class classification, the slightly lower binary classification performance suggests areas for refinement [5]. Future research should explore hybrid approaches combining amplitude-frequency sensitivity with topological insights [6], [10]. , integration of graph neural networks, and alternative graph construction methods such as visibility graphs or correlation-based networks. Extension to dark-adapted recordings, longitudinal studies, and multi-site validation would strengthen generalizability [16].

V. Conclusion

The ERG-Graph methodology represents a conceptual advancement by introducing topological analysis to ERG-based neurodevelopmental assessment. While not universally superior to traditional methods, it provides valuable complementary information for complex clinical scenarios and establishes a foundation for combining graph signal processing with physiological biomarkers. The approach could potentially extend to other electrophysiological signals, creating a comprehensive graph-based toolkit for neurodevelopmental assessment.

References

[1] M. J. Maenner *et al.*, "Prevalence and Characteristics of Autism Spectrum Disorder Among Children Aged 8 Years — Autism and Developmental Disabilities Monitoring Network, 11 Sites, United States, 2020," *MMWR Surveill. Summ.*, vol. 72, no. 2, pp. 1–14, Mar. 2023, doi: 10.15585/mmwr.ss7202a1.

[2] A. London, I. Benhar, and M. Schwartz, "The retina as a window to the brain—from eye research to CNS disorders," *Nat. Rev. Neurol.*, vol. 9, no. 1, pp. 44–53, Jan. 2013, doi: 10.1038/nrneurol.2012.227.

[3] P. A. Constable *et al.*, "Light-Adapted Electroretinogram Differences in Autism Spectrum Disorder," *J. Autism Dev. Disord.*, vol. 50, no. 8, pp. 2874–2885, Aug. 2020, doi: 10.1007/s10803-020-04396-5.

[4] I. O. Lee, D. H. Skuse, P. A. Constable, F. Marmolejo-Ramos, L. R. Olsen, and D. A. Thompson, "The electroretinogram b-wave amplitude: a differential physiological measure for Attention Deficit Hyperactivity Disorder and Autism Spectrum Disorder," *J. Neurodev. Disord.*, vol. 14, no. 1, p. 30, Dec. 2022, doi: 10.1186/s11689-022-09440-2.

[5] P. A. Constable *et al.*, "Spectral Analysis of Light-Adapted Electroretinograms in Neurodevelopmental Disorders: Classification with Machine Learning," *Bioengineering*, vol. 12, no. 1, p. 15, Dec. 2024, doi: 10.3390/bioengineering12010015.

[6] A. Ortega, P. Frossard, J. Kovačević, J. M. F. Moura, and P. Vandergheynst, "Graph Signal Processing: Overview, Challenges, and Applications," *Proc. IEEE*, vol. 106, no. 5, pp. 808–828, May 2018, doi: 10.1109/JPROC.2018.2820126.

[7] L. R. Mercado-Diaz, Y. R. Veeranki, F. Marmolejo-Ramos, and H. F. Posada-Quintero, "EDA-Graph: Graph Signal Processing of Electrodermal Activity for Emotional States Detection," *IEEE J. Biomed. Health Inform.*, vol. 28, no. 8, pp. 4599–4612, Aug. 2024, doi: 10.1109/JBHI.2024.3405491.

[8] A. Sandryhaila and J. M. F. Moura, "Discrete Signal Processing on Graphs," 2012, doi: 10.48550/ARXIV.1210.4752.

[9] *Practical Guide for Biomedical Signals Analysis Using Machine Learning Techniques*. Elsevier, 2019. doi: 10.1016/C2018-0-02414-7.

[10] D. I. Shuman, S. K. Narang, P. Frossard, A. Ortega, and P. Vandergheynst, "The emerging field of signal processing on graphs: Extending high-dimensional data analysis to networks and other irregular domains," *IEEE Signal Process. Mag.*, vol. 30, no. 3, pp. 83–98, May 2013, doi: 10.1109/MSP.2012.2235192.

[11] D. S. Bassett and O. Sporns, "Network neuroscience," *Nat. Neurosci.*, vol. 20, no. 3, pp. 353–364, Mar. 2017, doi: 10.1038/nn.4502.

[12] A. G. Robson *et al.*, "ISCEV Standard for full-field clinical electroretinography (2022 update)," *Doc. Ophthalmol.*, vol. 144, no. 3, pp. 165–177, Jun. 2022, doi: 10.1007/s10633-022-09872-0.

[13] P. A. Constable, S. B. Gaigg, D. M. Bowler, H. Jägle, and D. A. Thompson, "Full-field electroretinogram in autism spectrum disorder," *Doc. Ophthalmol.*, vol. 132, no. 2, pp. 83–99, Apr. 2016, doi: 10.1007/s10633-016-9529-y.

[14] "Electroretinograms in autism: a pilot study of b-wave amplitudes," *Am. J. Psychiatry*, vol. 145, no. 2, pp. 229–232, Feb. 1988, doi: 10.1176/ajp.145.2.229.

[15] N. N. J. Rommelse, B. Franke, H. M. Geurts, C. A. Hartman, and J. K. Buitelaar, "Shared heritability of attention-deficit/hyperactivity disorder and autism spectrum disorder," *Eur. Child Adolesc. Psychiatry*, vol. 19, no. 3, pp. 281–295, Mar. 2010, doi: 10.1007/s00787-010-0092-x.

[16] L. Lacasa, B. Luque, F. Ballesteros, J. Luque, and J. C. Nuño, "From time series to complex networks: The visibility graph," *Proc. Natl. Acad. Sci.*, vol. 105, no. 13, pp. 4972–4975, Apr. 2008, doi: 10.1073/pnas.0709247105.